HEAT TRANSFER ON SIMPLIFIED PRE-PERIOD STAGE OF TUNNEL FIRE

by

Hungwei LIU[a, b, c], Wei YAO[d*]

[a] Professional Engineer for CIVIL, Hong-Chu Construction Ltd., Taoyuan, Taiwan
[b] Department of Civil and Construction Engineering, National Taiwan University of Science and Technology, Taipei, Taiwan
[c] Department of Civil and Mineral Engineering, University of Toronto, Toronto, ON M5S 1A4, Canada
[d] State Key Laboratory of Hydraulics and Mountain River Engineering, College of Water Resource & Hydropower, Sichuan University, Chengdu, China

Tunnel fire is a part of applied thermal problems. With increase of transient temperature of the tunnel fire on the structure surface (i.e. tunnel lining), the heat transfer from the surface is possibly varying transient temperature distribution within the structure. The transient temperature distribution is also possibly damaging the composition of structure (micro-crack) because of critical damage temperature. Therefore, the transient temperature distribution has a significantly important role on defining mechanical and physical properties of structure and determining thermal-induced damaged region. The damage at pre-period stage of tunnel fire is perhaps more significant than that at the other period stages because of thermal gradient. Consequently, a theoretical model was developed for simplifying complicated thermal engineering during pre-period stage of tunnel fire. A hollow solid model (HSM) in a combination of dimensional analysis and heat transfer theory with Bessel's Function and Duhamel's Theorem were employed to verify a theoretical equation for dimensionless transient temperature distribution (DTTD) under linear transient thermal loading (LTTL). Experimental and numerical methods were also adopted to approve the results from this theoretical equation. The heating rate (M) is a primary variable for discussing DTTD on three means. The heating rate of 10.191, 10 and 240°C/min were applied to experimental and numerical studies. The experimental and numerical results are consistent with the theoretical solution, successfully verifying that the theoretical solution can predict the DTTD well in field. This equation can be used for thermal/tunnel engineers to evaluate the damaged region and to obtain the parameters related to DTTD.

Key words: *duhamel's theorem, dimensional analysis, temperature, transient thermal loading*

Introduction

Thermal engineering widely exists in the industry and the gradient of temperature possibly leads

[*]Corresponding author; e-mail: stevenyao84@163.com

to damage in structures and materials during the service period, such as the cylinder in vehicles (such as combustion chamber wall of Engine) [1], aerospace/petroleum structures [2], rock drilling [3], ore crushing, deep petroleum boring, geothermal energy extraction [4], deep burial of nuclear waste [5], carbon capture and storage [6, 7], tunnel fire [8, 9] (Figure 1), and electrical wire cover topic [10]. Those issues are directly related to heat transfer and temperature distribution in solids [9, 11, 12, 13, 14, 15, 16, 17]. Understanding the heat transfer process can predict and prevent the damage in solids during structure service period, which is significant for the structure safety. In addition, temperature increases rapidly and linearly up to thousands of Celsius degrees when a tunnel fire occurs and the heating rate is approximately 240°C/min. The high temperature on the surface of the structure or surround mass rock lasts during the entire tunnel fire period (Figure 2). However, the significant damage of tunnel and surround mass rock possibly occurs during the pre-period stage of tunnel fire, which is the heating stage shown as a red-dashed-line ellipse in Figure 2. The temperature on surface at heating stage is also called as outer transient temperature. Furthermore, the damage may be induced by thermal gradient which is from transient temperature distribution within the material body. It is worthy noted that the variety of temperature gradient in solids at the pre-period stage is more severe than that during the constant temperature stage. It is thus important to observe the transient temperature distribution within the body at the pre-period stage (heating stage M, of Figure 2) and predict the transient temperature distribution within the structures in many thermal engineering applications.

A myriad of researchers have discussed about thermal loading issues. Segall [18] studied thick-walled piping under polynomial transient thermal loading by using Duhamel's relationship. Shahani and Nabavi [19] provided an analytical temperature distribution solution for a thick-walled cylinder, the inner surface of which is subjected to time-dependent generalized thermal boundary conditions by using finite Hankel transform. Radu *et al.* [20] developed analytical solutions for temperature distribution in a hollow cylinder under sinusoidal transient thermal loading. Marie [21] proposed an extension of temperature and stress solution for a vessel or pipe under a linear shock or cyclic variation of fluid temperature and a simple analytical solution for thermal shock or cyclic variations of fluid temperature was found by using the linear shock resolution approach. Eraslan and Apatay [22] developed an analytical model for the prediction of thermal loading into a cylinder subjected to periodic boundary condition and the transient temperature distribution in the cylinder is obtained by using Duhamel's theorem. Although a lot of studies have been conducted for the temperature distribution of a hollow cylinder, the behavior of the temperature distribution of the hollow cylinder was not effectively compared and investigated using those approaches since a number of parameters exist in those models. Different models are not comparable when the parameters (e.g., inner and outer radius, thermal diffusivity, time, etc.) are changed. It is thus necessary to develop a mathematical model with dimensionless parameters, in which the non-dimensional temperature distribution with different parameters can be easily predicted and compared by engineers and industrial designers.

As mentioned above, in order to simulate the pre-period stage of tunnel fires (Figure 3), this paper aims to build a theoretical model for obtaining the dimensionless transient temperature distribution (DTTD) within Hollow-solid model (HSM) under linear transient thermal loading (LTTL) (Figure 3). The theoretical model is based on Heat Transfer theory under cylinder Coordinates [23, 24] and complies with Dimensional Analysis, Bessel's Function and Duhamel's Theorem. This model is verified by using experimental and numerical method. The paper is organized as follows. Dimensional analysis [25] is presented in Section 2, involving in the partial differential equation of heat conduction using Duhamel's theorem for temperature distribution [23]. Section 3 and 4 compare the results from theoretical solution with those from experimental and finite element method (FEM). Section 5 discusses the results. Conclusion is drawn in Section 6.

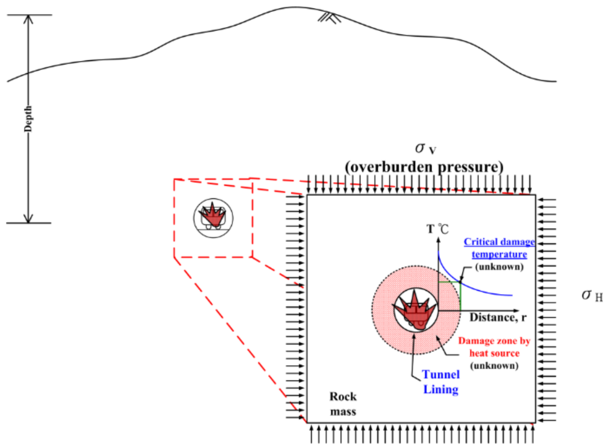

Figure 1. Temperature field in tunnel fire occurrence

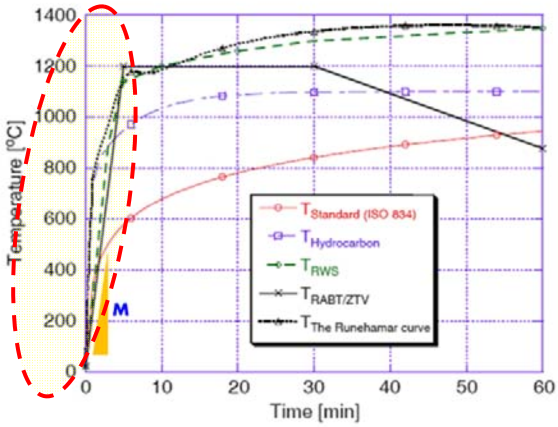

Figure 2. Temperature history in four different tunnel fire temperatures [8]

Dimensionless temperature distribution of a hollow solid under LTTL

Dimensional analysis is a useful tool to minimize the number of physical dimensional parameters in a mathematical model and to produce new equivalent dimensionless parameters. These new equivalent dimensionless parameters can be used to comprehensively analyze the problem and reduce experimental/numerical work [26]. Based on the dimensional analysis and the assumption of the identical temperature on the surface, the temperature distribution T (r, t) of HSM under LTTL can be expressed as:

$$T\left(r,t\right)=f\left(b,a,r,T_r,Mt,t,t_f,\alpha_P\right) \tag{1}$$

where b, a, and r are outer, inner, and arbitrary radius, respectively; T_r is room temperature, which is the model material's temperature in the unstrained state; Mt are initial temperature of linear transient thermal loading; t is arbitrary time and t_f is the time when the tensile or yield stress is larger than the tensile strength of solid; α_p is the thermal diffusivity of solid which is unchanged by around stresses.

LTS (length L, temperature T, and time S) unit system is adopted to analyze a, T, and t_f. The DTTD formula from Eq. (1) is rewritten as:

$$\frac{T\left(r/a,t\right)}{T_r}-1=f\left(\frac{b}{a},\frac{r}{a},\frac{Mt_f}{T_r}\frac{t}{t_f},\frac{t}{t_f},\frac{\alpha_P}{a^2}t_f\right) \tag{2}$$

or

$$\tilde{\theta}(\Gamma,\,t)=f\left(\Gamma_b,\,\Gamma,\,\tilde{M}\tilde{t},\,\tilde{t},\,\tilde{\alpha}_P\right) \tag{3}$$

where $\tilde{\theta}(\Gamma,\,\tilde{t})$ is the dimensionless temperature distribution of a hollow solid; Γ_b and Γ are the dimensionless outer and arbitrary radius, respectively; $\tilde{M}\tilde{t}$ is the dimensionless LTTL; $\tilde{M}$ is the dimensionless heating rate; $\tilde{t}$ is the dimensionless time; $\tilde{\alpha}_p$ is the dimensionless thermal diffusivity of solids.

The DTTD has to satisfy the heat diffusion equation within the cylinder coordination as follows,

$$\frac{\partial^2\tilde{\theta}}{\partial\Gamma^2}+\frac{1}{\Gamma}\frac{\partial\tilde{\theta}}{\partial\Gamma}=\frac{1}{\tilde{\alpha}_P}\frac{\partial\tilde{\theta}}{\partial\tilde{t}} \tag{4}$$

The temperature distribution is necessary to solve Eq. (4). The differential equations are the second order with respect to a single independent variable $\tilde{\theta}$. In the case of this study, the solution $\tilde{\theta}(\Gamma,\tilde{t})$ also satisfies two conditions: (a) Boundary condition ($\tilde{t}\geq 0$): The first boundary condition is the applied temperature on the internal hole surface of the structure at Γ=1. Thus,

$$\tilde{\theta}\left(1,\tilde{t}\right)=\tilde{M}\tilde{t}-1 \tag{5}$$

The second boundary condition of interest is the specified convection and radiation at $\Gamma=\Gamma_b$, it should yield,

$$\tilde{\theta}\left(\Gamma_b,\tilde{t}\right)=0 \tag{6}$$

where $\tilde{M}$ is assumed as a constant in pre-period stage of tunnel fire (Figure 2); (b) Initial condition

$(1 \le \Gamma \le \Gamma_b)$:

$$\tilde{\theta}(\Gamma, 0) = 0 \tag{7}$$

The $\tilde{\theta}(1, \tilde{t})$ is a known time-dependent function representing the thermal boundary condition applied on the internal hole surface of the structure.

The boundary and initial condition on the inner surface of a hollow cylinder solid can be measured or given through fire/temperature monitor in the structures. Thus, the DTTD under LTTL can be calculated by applying Duhamel's Theorem and Bessel's function.

According to Duhamel's Theorem, the surface of material under the HSM with LTTL is subjected to identical thermal boundary condition. Hence, it is addressed that a DTTD formula with a unit temperature from inner-hole surface (Γ=1) can be diffused by a variable, $\tilde{\phi}$, and Eq. (4) can be rewritten as

$$\frac{\partial^2 \tilde{\phi}}{\partial \Gamma^2} + \frac{1}{\Gamma}\frac{\partial \tilde{\phi}}{\partial \Gamma} = \frac{1}{\tilde{\alpha}_P}\frac{\partial \tilde{\phi}}{\partial \tilde{t}} \tag{8}$$

The above mentioned two conditions should be rewritten the following conditions for satisfying the Eq. (8): The boundary condition ($\tilde{t} \ge 0$):

$$\tilde{\phi}(1, \tilde{t}) = 1 \tag{9}$$

$$\tilde{\phi}(\Gamma_b, \tilde{t}) = 0 \tag{10}$$

and the initial condition $(1 \le \Gamma \le \Gamma_b)$:

$$\tilde{\phi}(\Gamma, 0) = 0 \tag{11}$$

However, because the boundary condition mentioned above is a non-homogeneous boundary conditions, the boundary cannot be solved on mathematical method, it should be transferred to a homogenous boundary condition. Therefore, the $\tilde{\phi}(\Gamma, \tilde{t})$ is partitioned into two parts as follows,

$$\tilde{\phi}(\Gamma, \tilde{t}) = U(\Gamma, \tilde{t}) + \psi(\Gamma) \tag{12}$$

where $U(\Gamma, \tilde{t})$ and ψ (Γ) are location-time function and geometrical function, respectively. The function ψ (Γ) can be obtained as follows

$$\psi(\Gamma) = \frac{\ln(\Gamma_b/\Gamma)}{\ln(\Gamma_b)} \tag{13}$$

Assuming $U(1, \tilde{t}) = U(\Gamma_b, \tilde{t}) = 0$, $U(\Gamma, 0) = -\psi(\Gamma)$, then

$$U(\Gamma, \tilde{t}) = R_v(\Gamma) T_t(\tilde{t}) \tag{14}$$

where $R_v(\Gamma)$ and $T_t(\tilde{t})$ are related to the geometrical function and time domain function. Consequently, $T_t(\tilde{t})$ is substituted into Eq. (14) to rewrite the boundary as a homogeneous boundary conditions and the following initial condition

$$U(\Gamma, 0) = \sum_{m=1}^{\infty} C_m R_0(\beta_m, \Gamma) = -\psi(\Gamma) \tag{15}$$

Based on the heat transfer theory [23], C_m and $R_0(\beta_m, \Gamma)$ can be obtained here and β_m is the positive roots of transcendental equation (m=1.2,3,…). Thus, a DTTD diffusing formula with a unit temperature within the solid from inner-hole surface can be obtained as follows,

$$\tilde{\phi}(\Gamma, \tilde{t}) = \frac{\ln\left(\Gamma_b / \Gamma\right)}{\ln(\Gamma_b)} - \frac{\pi^2}{2}\sum_{m=1}^{\infty} \beta_m^{\ 2} \frac{J_0^{\ 2}(\beta_m)}{\begin{vmatrix} J_0(\beta_m) & J_0(\beta_m \Gamma_b) \\ J_0(\beta_m \Gamma_b) & J_0(\beta_m) \end{vmatrix}} \times e^{-\beta_m^2 \tilde{\alpha}_P \tilde{t}} \begin{vmatrix} J_0(\beta_m \Gamma) & J_0(\beta_m \Gamma_b) \\ Y_0(\beta_m \Gamma) & Y_0(\beta_m \Gamma_b) \end{vmatrix} \int_1^{\Gamma_b} \Gamma \begin{vmatrix} J_0(\beta_m \Gamma) & J_0(\beta_m \Gamma_b) \\ Y_0(\beta_m \Gamma) & Y_0(\beta_m \Gamma_b) \end{vmatrix} \frac{\ln\left(\Gamma_b / \Gamma\right)}{\ln(\Gamma_b)} d\Gamma \tag{16}$$

According to the Duhamel's theorem [18, 22, 23, 27] for LTTL, the dimensional approaching solution of DTTD obtained by imposing Eq. (6) and Eq. (16) is given by

$$\tilde{\theta}(\Gamma, \tilde{t}) = \Theta(\chi - \eta) \tag{17}$$

where $\Theta = \dfrac{\tilde{M}}{\ln(\Gamma_b)}$, $\chi = \ln\left(\dfrac{\Gamma_b}{\Gamma}\right)\tilde{t}$, $\eta = \dfrac{\pi^2}{2}\sum_{m=1}^{\infty}\left\{ J_0^{\ 2}(\beta_m) \dfrac{\begin{vmatrix} J_0(\beta_m \Gamma) & J_0(\beta_m \Gamma_b) \\ Y_0(\beta_m \Gamma) & Y_0(\beta_m \Gamma_b) \end{vmatrix}}{\begin{vmatrix} J_0(\beta_m) & J_0(\beta_m \Gamma_b) \\ J_0(\beta_m \Gamma_b) & J_0(\beta_m) \end{vmatrix}} \times \dfrac{1}{\tilde{\alpha}_p}\left[1 - e^{-\beta_m^{\ 2}\tilde{\alpha}_p \tilde{t}}\right] \times \sum_{\Gamma=1}^{\Gamma=\Gamma_b} \Gamma \begin{vmatrix} J_0(\beta_m \Gamma) & J_0(\beta_m \Gamma_b) \\ Y_0(\beta_m \Gamma) & Y_0(\beta_m \Gamma_b) \end{vmatrix} \ln\left(\dfrac{\Gamma_b}{\Gamma}\right)\Delta\Gamma \right\}\Bigg\}$.

$\Theta\chi$ is the DTTD at any instantaneous time at steady-state heat conduction; $\Theta\eta$ is the DTTD at whichever instantaneous time at unsteady-state heat conduction.

As a result, the diffusing solution of DTTD under LTTL from the inner-hole surface was defined by steady-state function minus unsteady-state function in certain time. For arbitrary transient thermal loading, Eq. (3) and Eq. (8) can be used to calculate the corresponding DTTD.

Experimental study

In this study, the cement-based solid (mortar) is adopted to verify the theoretical equation of DTTD with LTTL. Components of the mortar were as follows. Matrix is made from Type-I Portland cement, which is produced from the Taiwan Cement Corporation. A natural crystalline quartz (high purity (99% SiO_2)) with a uniform gain (fine and coarse sand diameter range from 0.718 to 1.19 mm; D_{50}=1.0 mm). The mixture proportion of the cement, water, and sand is 1:0.5:2.75. The HSM with LTTL tests were conducted on square-shaped specimen, which was prepared with Length×Height×Width = 140×140×50 mm and a circular hole with 20 mm diameter in the center of the specimen. The thermal diffusivity coefficient of mortar (α_p) after curing 28-day in water is 1.23×10^{-6} (m^2/s). To eliminate the effect of pore-water on the temperature distribution measurement, the mortar specimen was heated at 105°C in the furnace before the experiment. The heating rate (2°C/min) in the furnace is slow enough to avoid the thermal-induced stress in the specimen. The chemical change of cement-based material is not considered in this study because the temperature is lower than the critical temperature for the chemical change.

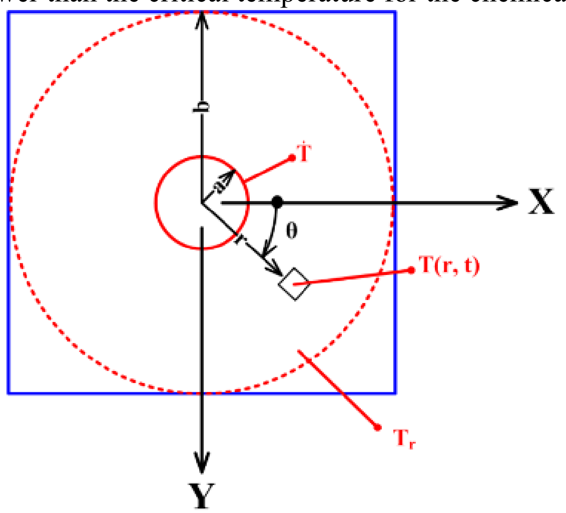

Figure 3. Hollow solid with transient thermal loading model

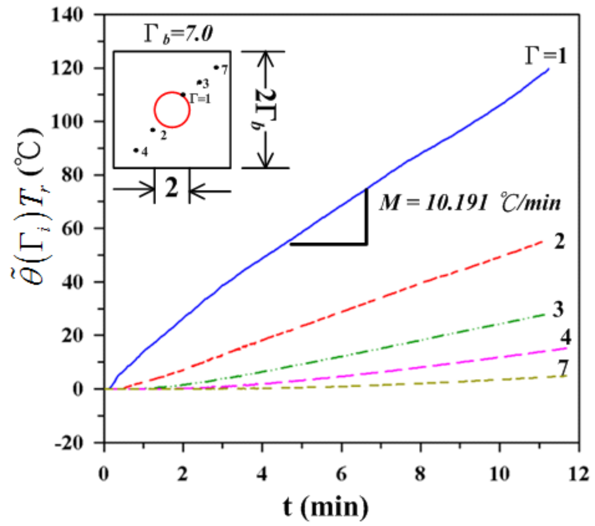

Figure 4. The temperature history for each themo-couple measurement position

A heating bar in the circular hole was applied to heating the specimen. The heating rate capacity and the highest temperature of the heating bar are approximately 10 to 30°C/min and 350°C, respectively. For measuring the temperature distribution within specimen, five thermo-couple points are chosen in the specimen. Because of a nonlinear temperature distribution, the locations of these points are chosen as Figure 4 and marked as 1, 2, 3, 4, and 7. Each thermo-couple was arranged in a half of width of specimen (25 mm). The measuring device of the thermocouples includes a measurement system (NI-9213) and controlling software (LabVIEW program) developed by the Nation Instrument Company. This high-density thermocouple measurement device designed for higher-channel-count bus-powered systems was adopted for measuring and recording the temperature and the measuring error of the thermocouples and device is lower than 3~4°C.

The temperature of the bar on the inner-hole surface (Γ=1) is from room temperature (T_r=26°C) to the critical temperature (T_f=102°C), which is addressed by fracture occurrences in the specimen. The heating lasted approximately 7 minutes. It is noted that the fracture occurrence means that the maximum tensile stress in the certain location of the specimen is equal to the tensile strength of the material. Thus, at least a primary crack was produced at the certain location of the material, leading to the transform from continuous to discontinuous deformation. Further, the heating rate (M) is approximately 10.191°C/min (Figure 4). In addition, the temperature history at each of thermo-couple position was illustrated in Figure 4. Each measured temperature at the time of fracture occurrence and the DTTD derived from the theoretical approach are shown in Figure 6.

Numerical analysis

In this study, the DTD of HSM with LTTL was simulated using an explicit non-linear finite element code, ABAQUS/Standard software. In this simulation, the temperature on the surface of structure solid and heat transfer within the structure solid was considered. An element component of thermal-mechanical element (*C3D8T*) was applied to the HSM with LTTL. The *C3D8T* element is a coupled displacement-temperature 8 nodes solid element, which are Gauss integration points. Such solid element is known to present some locking behavior, both shear and volumetric locking [28]. The HSM with LTTL simulation was conducted on a half square-shaped model with Length×Height×Width = 2×1×0.001 m and a half of circular hole with 2 cm diameter in the center of the model, as shown in Figure 5. Based on the mesh sensitivity analysis, the element distribution was selected as 35048 elements in the half of simulation model with the mesh segmentation using radial reflection with magnification of 1.03 times.

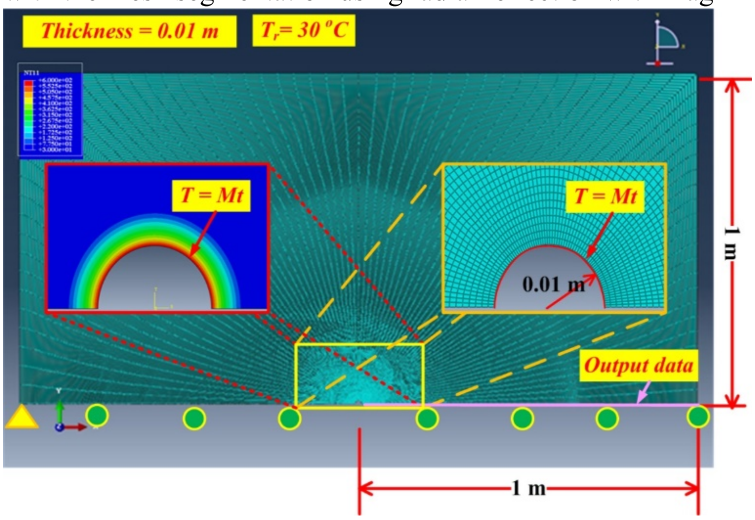

Figure 5. Geometry, mesh segmentation, boundary and initial conditions, and the positions of output data of numerical method

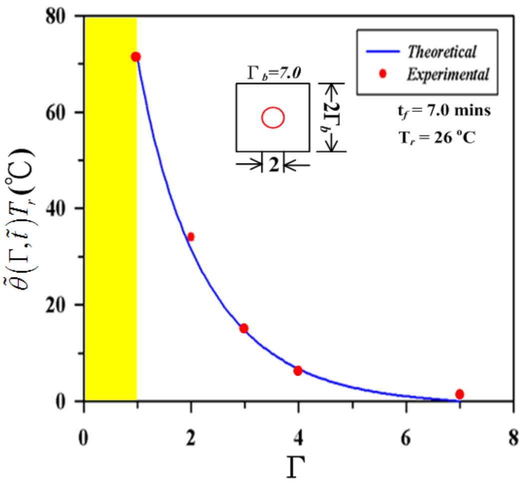

Figure 6. Temperature distribution at brittle fracture of material from the theory and the experiment when M= 10.191°C/min

Thermal diffusivity coefficient of the rock material is 0.68×10^{-6} (m^2/s) into the simulation model for analyzing the DTTD. It is noted that this coefficient for rocks was genrally in the range between approximate 0.68×10^{-6} and 1.5×10^{-6} (m^2/s). The initial temperature in the whole model is 30°C. Two heating rates (M) on internal hole surface were simulated, i.e., 10°C/min and 240°C/min for Γ_b=100. The 10°C/min and 240°C/min are used in both the experiments and the simulations for the case of tunnel fire (Figure 2), respectively. The both cases are employed to verify the theoretical DTTD equation. The temperature on the surface increases from 30 to 600°C. The maximum temperature in the simulation is discussed because the critical damaged temperature of the rock and cement-based material is usually in the range of 450 and 550°C [11, 29, 30, 31, 32]. The numerical simulation result and the theoretical curves for these two cases are shown in Figure 7 and Figure 8, respectively. The thermal engineers and designers can follow the temperature distribution of the materials (i.e., rock and cement-based material) in this study to assess the thermal-induced damage region for the design and repair period of structures.

Discussions

The accuracy of the numerical and analytical solutions for the temperature response significantly depend on the size of the incremental step in the Γ. Due to the application of the complex mathematical series expansions, the solutions are exhibited as discrete points. Therefore, a smoothing technique based on the polynomial fitting of analytical distributions are used in this study [20]. In addition, the number of Bessel's roots (β_m) has been checked for obtaining the right analytical solutions. In this study, the analytical DTTD solution and the DTTD from experiments are compared at the same heating rate for verifying the theoretical equations for solving the DTTD. In the experiments, the heating rate and the time of brittle fracture occurrence are 10.191°C/min and about 7 minutes, respectively. At the same heating rate and heating period, the analytical DTTD solutions (i.e., $\tilde{\theta}\left(\Gamma_b,\ \tilde{t}\right)\times T_r$) were also calculated utilizing the numeric computing method through *MATLAB*. In addition, the theoretical temperature distribution is shown as a blue line in Figure 6, and the temperatures at the time of brittle fracture occurrence for measurement positions in Figure 4 are illustrated as red dots in Figure 6. It indicates that the results from the experimental measurement (red points) and the theoretical approach (blue line) have a good agreement, verifying that the theoretical method proposed in this study is valid to predict the DTTD of HSM with LTTL.

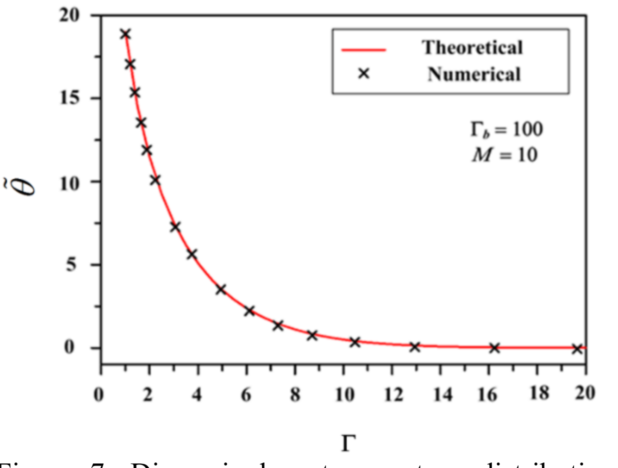

Figure 7. Dimensionless temperature distribution with M=10°C/min

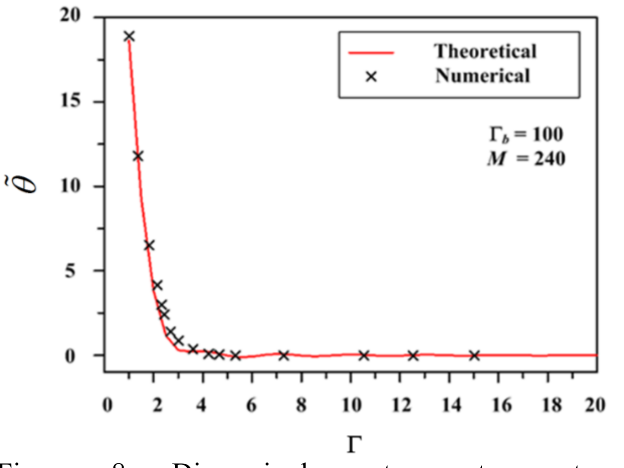

Figure 8. Dimensionless temperature stress distribution with M=240°C/min

Moreover, the numerical simulation is conducted with two heating rates: 10°C/min and 240°C/min. Meanwhile, these two heating rates and the time of receiving 600°C were substituted into the numeric computing program of theoretical approach to obtain the DTTD ($\tilde{\theta}$), which is shown as a red line in Figure 7 (M=10°C/min) and Figure 8 (M=240°C/min), respectively. The results derived from the numerical simulation are shown as black cross in both Figs. 7 and 8. The comparison between the results from the numerical simulation (black cross) and the theoretical approach (red line) indicates that the results from these two methods are consistent. As a result, the validity of the theoretical approach for calculating the DTTD of HSM with LTTL is approved.

Conclusions

Tunnel fire is a complex thermal engineering problem. A simplified theoretical approach for the DTTD of HSM with LTTL is proposed to obtain the temperature distribution during the pre-period stage of the tunnel fire. The dimensional analysis, Bessel's function and Duhamel's theorem are successfully used to achieve the theoretical equation for solving the DTTD. In this theoretical approach, only five variables need to be considered to calculate the temperature distribution during the heat transfer under linear transient thermal loading. In addition, the theoretical solutions are compared with the results derived from both experimental and numerical methods. All the results obtained from the theoretical prediction, the experimental measurement, and the numerical simulation at the same initial and boundary conditions are consistent. This successfully verifies that the simplified theoretical approach proposed in this study can predict the DTTD under LTTL well in field. Furthermore, the theoretical equation is valid for both the different initial and boundary conditions and the various material properties (e.g., the thermal diffusivity coefficient, the geometry of structures), and thus can be also applied to the industrial design and thermal engineering, such as the electrical wire design and nuclear waste storage. Moreover, the damaged region within the structures may be determined by using the temperature distribution derived from this theoretical approach.

Acknowledgements

The authors would like to express his appreciation to Peiwun Shih and Yihung Liu for their help in the operations of this study, respectively. This work was supported by State Key Laboratory of Hydraulics and Mountain River Engineering (SKHL) (Grant No. SKHL1606).

References

[1] Enomoto, Y., Furuhama, S., Study on Thin Film Thermocouple for Measuring Instantaneous Temperature on Surface of Combustion Chamber Wall in Internal Combustion Engine, *Bulletin of JSME*, 28 (1985), 235, pp. 108-116

[2] Malekan, M., *et al.*, Thermo-Mechanical Analysis of a Cylindrical Tube under Internal Shock Loading Using Numerical Solution, *Journal of the Brazilian Society of Mechanical Sciences and Engineering*, 38 (2016), 8, pp. 2635-2649

[3] Menezes, P. L., Influence of Cutter Velocity, Friction Coefficient and Rake Angle on the Formation of Discontinuous Rock Fragments During Rock Cutting Process, *The International Journal of Advanced Manufacturing Technology*, 90 (2017), 9, pp. 3811-3827

[4] Cao, P., *et al.*, Experimental Investigation of Cutting Temperature in Ice Drilling, *Cold Regions Science and Technology*, 116 (2015), pp. 78-85

[5] Fox, D. B., *et al.*, Sustainable Heat Farming: Modeling Extraction and Recovery in Discretely Fractured Geothermal Reservoirs, *Geothermics*, 46 (2013), pp. 42-54

[6] Vilarrasa, V., *et al.*, Hydromechanical Characterization of Co_2 Injection Sites, *International Journal of Greenhouse Gas Control*, 19 (2013), pp. 665-677

[7] Gor, G. Y., *et al.*, Effects of Thermal Stresses on Caprock Integrity During Co_2 Storage, *International Journal of Greenhouse Gas Control*, 12 (2013), pp. 300-309

[8] Lönnermark, A., Ingason, H., Gas Temperatures in Heavy Goods Vehicle Fires in Tunnels, *Fire Safety Journal*, 40 (2005), 6, pp. 506-527

[9] Pichler, C., *et al.*, Safety Assessment of Concrete Tunnel Linings under Fire Load, *Journal of Structural Engineering*, 132 (2006), 6, pp. 961-969

[10] Brito Filho, J. P., Heat Transfer in Bare and Insulated Electrical Wires with Linear

Temperature-Dependent Resistivity, *Applied Thermal Engineering*, 112 (2017), pp. 881-887
[11] Liu, H., *et al.*, Suggested Continued Heat-Treatment Method for Investigating Static and Dynamic Mechanical Properties of Cement-Based Materials, *Construction and Building Materials*, 69 (2014), pp. 91-100
[12] Yu, J., *et al.*, Residual Fracture Properties of Concrete Subjected to Elevated Temperatures, *Materials and Structures*, 45 (2012), 8, pp. 1155-1165
[13] He, Z. J., Song, Y. P., Triaxial Strength and Failure Criterion of Plain High-Strength and High-Performance Concrete before and after High Temperatures, *Cement and Concrete Research*, 40 (2010), 1, pp. 171-178
[14] Peng, G. F., *et al.*, Explosive Spalling and Residual Mechanical Properties of Fiber-Toughened High-Performance Concrete Subjected to High Temperatures, *Cement and Concrete Research*, 36 (2006), 4, pp. 723-727
[15] Yu, K., Lu, Z., Determining Residual Double-K Fracture Toughness of Post-Fire Concrete Using Analytical and Weight Function Method, *Materials and Structures*, 47 (2014), 5, pp. 839-852
[16] Zhang, Z. Z., *et al.*, Effect of Thermal Treatment on Fractals in Acoustic Emission of Rock Material, *Advances in Materials Science and Engineering*, 2016 (2016), pp. 1-9
[17] Zhang, Y., *et al.*, An Experimental Investigation of Transient Heat Transfer in Surrounding Rock Mass of High Geothermal Roadway, *Thermal Science*, 20 (2016), 6, pp. 2149-2158
[18] Segall, A. E., Transient Analysis of Thick-Walled Piping under Polynomial Thermal Loading, *Nuclear Engineering and Design*, 226 (2003), 3, pp. 183-191
[19] Shahani, A. R., Nabavi, S. M., Analytical Solution of the Quasi-Static Thermoelasticity Problem in a Pressurized Thick-Walled Cylinder Subjected to Transient Thermal Loading, *Applied Mathematical Modelling*, 31 (2007), 9, pp. 1807-1818
[20] Radu, V., *et al.*, Development of New Analytical Solutions for Elastic Thermal Stress Components in a Hollow Cylinder under Sinusoidal Transient Thermal Loading, *International Journal of Pressure Vessels and Piping*, 85 (2008), 12, pp. 885-893
[21] Marie, S., Analytical Expression of the Thermal Stresses in a Vessel or Pipe with Cladding Submitted to Any Thermal Transient, *International Journal of Pressure Vessels and Piping*, 81 (2004), 4, pp. 303-312
[22] Eraslan, A. N., Apatay, T., Analytical Solution to Thermal Loading and Unloading of a Cylinder Subjected to Periodic Surface Heating, *Journal of Thermal Stresses*, 39 (2016), 8, pp. 928-941
[23] Özişik, M. N., *Heat Conduction*, Wiley, New York, USA, 1993
[24] Zhang, J. G., The Fourier-Yang Integral Transform for Solving the 1-D Heat Diffusion Equation, *Thermal Science*, 21 (2017), 1, pp. S63-S69
[25] Barenblatt, G. I., *Dimensional Analysis*, CRC Press, Boca Raton, USA, 1987
[26] Chen, L. H., Failure of Rock under Normal Wedge Indentation: Civil & Mineral Engineering, Ph. D. thesis, University of Minnesota, Minneapolis, USA, 2001
[27] Krishnamurthy, H., Application of Duhamel's Theorem to Problems Involving Oscillating Heat Source, M. SC. thesis, *Bangalore University, Bengaluru, India*, 2002
[28] Haddag, B., *et al.*, Finite Element Formulation Effect in Three-Dimensional Modeling of a Chip Formation During Machining, *International Journal of Material Forming*, 3 (2010), 1, pp. 527-530
[29] Yao, W., *et al.*, Quantification of Thermally Induced Damage and Its Effect on Dynamic Fracture Toughness of Two Mortars, *Engineering Fracture Mechanics*, 169 (2017), pp. 74-88
[30] Mahanta, B., *et al.*, Influence of Thermal Treatment on Mode I Fracture Toughness of Certain Indian Rocks, *Engineering Geology*, 210 (2016), pp. 103-114
[31] Yin, T., *et al.*, Effect of Thermal Treatment on the Dynamic Fracture Toughness of Laurentian Granite, *Rock Mechanics and Rock Engineering*, 45 (2012), 6, pp. 1087-1094
[32] Chaki, S., *et al.*, Influence of Thermal Damage on Physical Properties of a Granite Rock: Porosity, Permeability and Ultrasonic Wave Evolutions, *Construction and Building Materials*, 22 (2008), 7, pp. 1456-1461

Paper submitted: Auguest 10, 2018

Paper revised: Auguest 29, 2018

Paper accepted: December10, 2018